

B_K with improved staggered fermions: analysis using SU(2) staggered chiral perturbation theory

Boram Yoon*, Taegil Bae, Yong-Chull Jang, Hyung-Jin Kim, Jangho Kim, Jongjeong Kim, Kwangwoo Kim, Weonjong Lee

Lattice Gauge Theory Research Center, CTP, and FPRD,

Department of Physics and Astronomy, Seoul National University, Seoul, 151-747, South Korea

E-mail: wlee@snu.ac.kr

Chulwoo Jung

Physics Department, Brookhaven National Laboratory, Upton, NY11973, USA

E-mail: chulwoo@bnl.gov

Stephen R. Sharpe

Physics Department, University of Washington, Seattle, WA 98195-1560

E-mail: sharpe@phys.washington.edu

We report updated results for B_K calculated using HYP-smearred staggered fermions on the MILC asqtad 2 + 1 flavor lattices. We use four different lattice spacings ($a \approx 0.12, 0.09, 0.06$ and 0.045 fm) to control the continuum extrapolation. We use SU(2) staggered chiral perturbation theory to do the data analysis. We find that $B_K(\text{NDR}, \mu = 2 \text{ GeV}) = 0.526 \pm 0.007 \pm 0.024$ and $\hat{B}_K = B_K(\text{RGI}) = 0.720 \pm 0.010 \pm 0.033$. Here the first error is statistical and the second systematic. The dominant source of error is that due to our use of a truncated (one-loop) matching factor.

The XXVIII International Symposium on Lattice Field Theory, Lattice2010

June 14-19, 2010

Villasimius, Italy

*Speaker.

1. Introduction

This is the first of four proceedings providing an update of our calculation of B_K using improved staggered fermions (HYP-smearred valence quarks on the MILC asqtad lattices). Here we present results using fits based on SU(2) staggered chiral perturbation theory (SChPT), the method that leads to our most accurate results. We focus on the progress made since last year's lattice proceedings, Ref. [1]. The other proceedings present, respectively, results using fits based on SU(3) SChPT [2], a study of some sources of error [3], and a more detailed look at results from the ultrafine ensemble [4].

Table 1 shows the present status of our running. In the last year, we increased the number of measurements on the C4 and S1 ensembles (by factors of 10 and > 2 , respectively), and added two new ensembles: F2 and U1. The F2 ensemble allows us to further check the sea-quark mass dependence, while the U1 ensemble provides a fourth lattice spacing. We have also written a long article, Ref. [5], in which we explain both the SU(2) and SU(3) SChPT calculations leading to our fitting forms, describe our fitting methods, and present our full error budget. The results presented in Ref. [5] are intermediate between those presented at last year's lattice conference [1] and those presented here. In particular, Ref. [5] does not include results from the U1 ensemble.

a (fm)	am_l/am_s	geometry	ID	ens \times meas	$B_K(\mu = 2 \text{ GeV})$	status
0.12	0.03/0.05	$20^3 \times 64$	C1	564×1	0.557(14)	old
0.12	0.02/0.05	$20^3 \times 64$	C2	486×1	0.569(16)	old
0.12	0.01/0.05	$20^3 \times 64$	C3	671×9	0.565(5)	old
0.12	0.01/0.05	$28^3 \times 64$	C3-2	275×8	0.570(5)	old
0.12	0.007/0.05	$20^3 \times 64$	C4	651×10	0.562(5)	update
0.12	0.005/0.05	$24^3 \times 64$	C5	509×1	0.554(11)	old
0.09	0.0062/0.031	$28^3 \times 96$	F1	995×1	0.544(12)	old
0.09	0.0031/0.031	$40^3 \times 96$	F2	678×1	0.547(10)	new
0.06	0.0036/0.018	$48^3 \times 144$	S1	744×2	0.539(7)	update
0.045	0.0028/0.014	$64^3 \times 192$	U1	305×1	0.527(11)	new

Table 1: MILC asqtad ensembles used to calculate B_K . $B_K(\text{NDR}, 2 \text{ GeV})$ is obtained using the SU(2) analysis with 4X3Y-NNLO fits (discussed in the text).

2. SU(2) SChPT Analysis

Our analysis makes essential use of SChPT [6, 7] in order to remove artifacts associated with taste breaking. The application of SChPT to B_K was worked out for SU(3) SChPT in Ref. [8]. The extensions to our mixed-action set-up, and to SU(2) ChPT, were presented in Ref. [5]. We summarize the findings of the latter work in this section.

SU(2) ChPT treats the strange quark as heavy, and expands in m_π^2/m_K^2 , as well as in the usual ratio m_π^2/Λ_χ^2 (with $\Lambda_\chi \sim 1 \text{ GeV}$) [9, 10]. It has been argued that this is a more reliable way of extrapolating kaon properties to the physical quark masses than using SU(3) ChPT, in which the strange quark is treated as light. Whether or not this is true in general, it turns out that, for our

application, there is an additional important advantage of SU(2) ChPT. This is that, at next-to-leading-order (NLO), the SU(2) SChPT expression contains no low-energy coefficients (LECs) arising from discretization or truncation errors.¹ This is not the case in SU(3) ChPT, and, as a result, the latter gives rise to cumbersome fitting forms with many parameters. In SU(2) SChPT, by contrast, one has the same number of parameters at NLO as for a fermion discretization with chiral symmetry, such as domain-wall fermions. We find [5]

$$f_{\text{th}} = d_0 F_0 + d_1 \frac{X_P}{\Lambda_\chi^2} + d_2 \frac{X_P^2}{\Lambda_\chi^4} + d_3 \frac{L_P}{\Lambda_\chi^2} \quad (2.1)$$

where the chiral logs reside in the function

$$F_0 = 1 + \frac{1}{32\pi^2 f_\pi^2} \left\{ \ell(X_I) + (L_I - X_I) \tilde{\ell}(X_I) - 2\langle \ell(X_B) \rangle \right\} \quad (2.2)$$

$$\langle \ell(X_B) \rangle = \frac{1}{16} \left[\ell(X_I) + \ell(X_P) + 4\ell(X_V) + 4\ell(X_A) + 6\ell(X_T) \right]. \quad (2.3)$$

$$\ell(X) = X \left[\log(X/\mu_{\text{DR}}^2) \right], \quad \tilde{\ell}(X) = -d\ell(X)/dX \quad (2.4)$$

Here X_B (L_B) is the squared mass of the valence (sea) pion with taste B, which we know from our simulations or those of the MILC collaboration. It is only through these masses that the taste-breaking enters at NLO. The coefficients d_i have an unknown dependence on $r_s = m_s/\Lambda_{\text{QCD}}$, and, in addition, d_0 is a function of a^2 and α_s^2 .

We have included an analytic NNLO term in Eq. 2.1, with coefficient d_2 , and we do fits both without and with this term, labeled respectively as NLO and NNLO. The latter fits are not full NNLO fits, but rather are used to gauge the errors arising from truncating ChPT.

3. Fitting and Results

Our lattice kaon is composed of valence (anti)quarks with masses m_x and m_y , which are to be extrapolated to m_d^{phys} and m_s^{phys} , respectively. On each lattice we use 10 valence masses:

$$am_x, am_y = am_s \times n/10 \quad \text{with} \quad n = 1, 2, 3, \dots, 10,$$

where am_s is the strange sea-quark mass (which lies fairly close to the physical strange mass). For our standard SU(2) fitting we choose the lowest 4 values for am_x and the highest 3 values for am_y , calling the resulting fits “4X3Y”. This means that we use only 12 out of the possible 55 mass combinations, but by doing so we maintain the SU(2) condition $m_x/m_y \ll 1$.

We do the fitting in two stages. First, for fixed m_y , we fit the m_x (or, equivalently, X_P) dependence to the form (2.1). We call this the “X-fit”, examples of which are shown in Fig. 1. This fit allows us to extrapolate $m_x \rightarrow m_d^{\text{phys}}$ and to remove taste-breaking discretization and perturbative truncation errors by setting $X_I = X_B = X^{\text{phys}}$ in Eq. (2.2). We can also partially correct for the use of an unphysical m_ℓ by setting L_I to its physical value. The result of this procedure is shown in the figures by the red points.

¹Truncation errors arise because we match the four-fermion operator appearing in B_K to continuum regularization using one-loop perturbation theory.

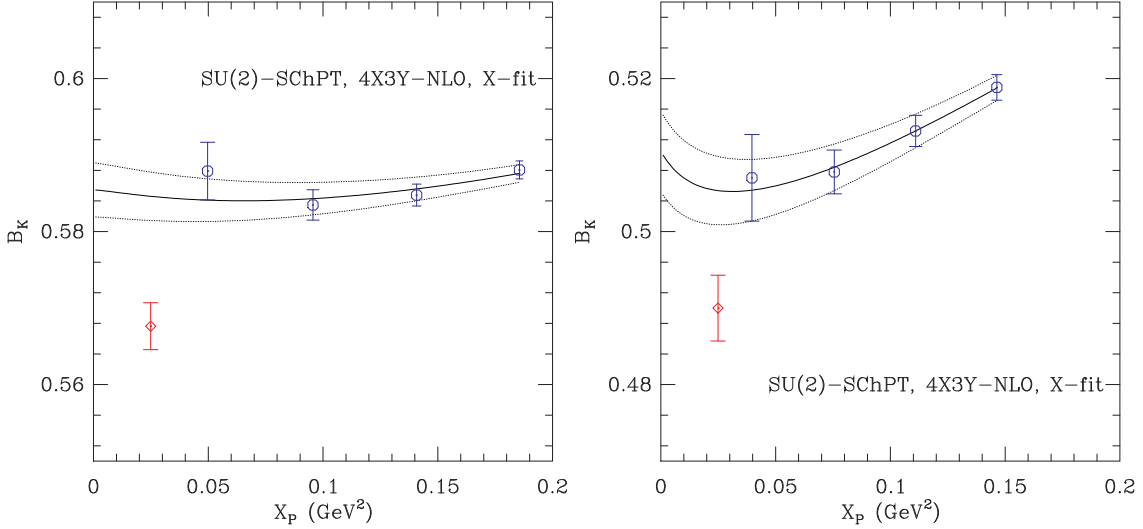


Figure 1: 4X-NLO fit of B_K versus X_P for the C3 (left) and S1 (right) ensembles. The red point gives the physical result, as discussed in the text. Here, we fix $am_y = 0.05$ for C3 and $am_y = 0.018$ for S1.

In the second stage, we extrapolate the corrected points from the 3 values of m_y to m_s^{phys} . The dependence here is analytic, and we use both linear and quadratic forms in these “Y-fits”. The Y-fits are straightforward, and we refer to Ref. [5] for examples. Here we focus on the X-fits.

ID (meas)	d_0	d_1	d_2	$\chi^2/\text{d.o.f}$
C3 (671 × 9)	0.5602(34)	0.035(16)	—	0.83(54)
S1 (744 × 2)	0.4808(50)	0.143(30)	—	0.06(14)
S1 (513)	0.469(15)	0.33(21)	-0.72(81)	0.002(18)
S1 (744 × 2)	0.4834(93)	0.09(13)	0.27(51)	0.075(94)

Table 2: Parameters of X-fits shown in Figs. 1 and 3.

The parameters of the fits shown in Fig. 1 are given in the first two rows of Table 2.² We use uncorrelated fits and thus expect $\chi^2/\text{d.o.f} \ll 1$ for a good fit. The C3 data are unchanged from last year (Refs. [1, 5]) while the S1 results have significantly improved statistics. The curvature in these NLO fit functions is entirely due to the chiral logarithms, and is consistent with our data on all ensembles. The convergence of the chiral expansion can be gauged from the difference between the values of d_0 in the Table (which is the LO result) and the results in the figures. The ratio of NLO to LO terms is $< 10\%$ for all points used in the fits. Such satisfactory convergence is seen on all other ensembles [5].

The rather large χ^2 in the C3 fit may be indicative of the need to include NNLO terms, and indeed the χ^2 of our NNLO fit is much reduced. The resulting extrapolated-corrected value of B_K (the red point) is, however, very similar in both fits.

In Fig. 2, we compare 4X-NLO fits on the F1 and F2 lattices. The former results are from last year, while the latter are new. These two ensembles differ only in the value of light sea-quark mass,

²For a given ensemble with fixed am_l , d_3 is absorbed into d_0 .

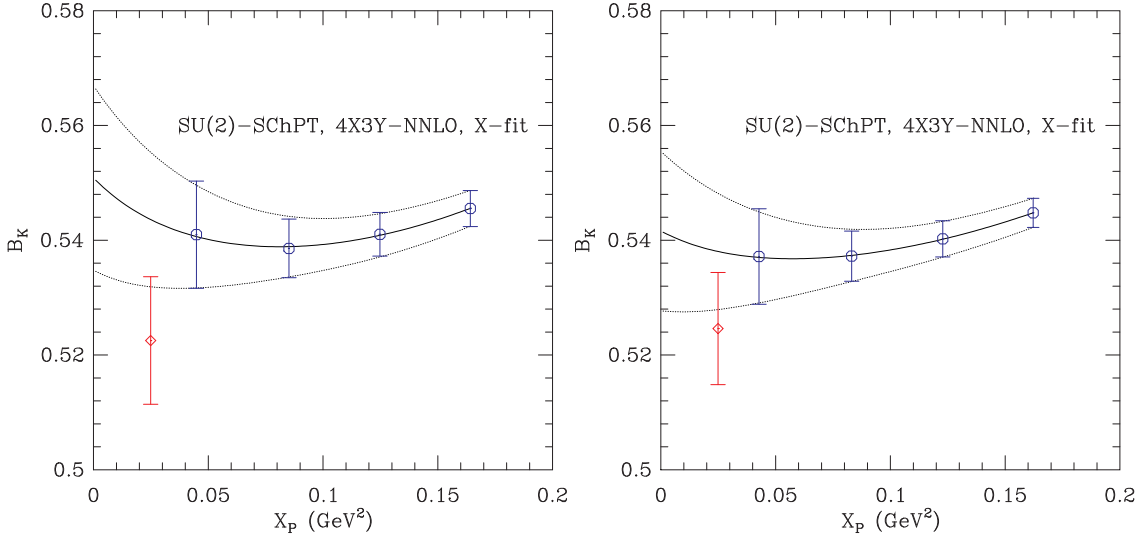


Figure 2: B_K versus X_P on the F1 (left) and F2 (right) ensembles, showing a 4X3Y-NNLO fit. Notation as in Fig. 1. Here, we set $am_y = 0.031$ for both F1 and F2.

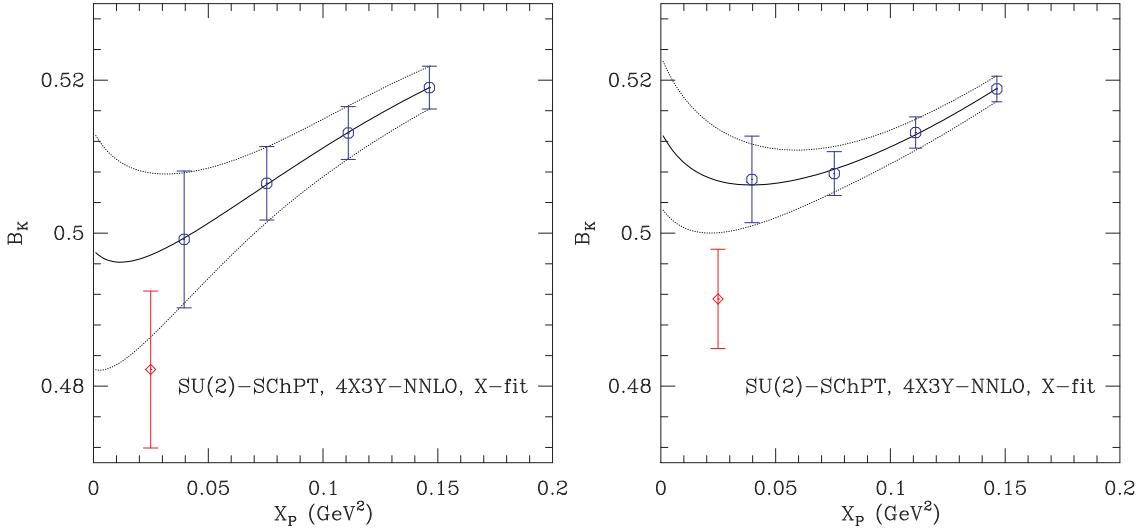


Figure 3: B_K versus X_P on S1 ensemble for 513 configurations (left) and for 744 configurations \times 2 measurements (right). The plots are for $am_y = 0.018$. 4X3Y-NNLO fits are shown. Notation as in Fig. 1.

and we see that results are very similar on the two ensembles. This can be seen quantitatively from the resulting values of $B_K(2 \text{ GeV})$ given in Table 1. The lack of dependence on am_ℓ confirms the result found on the coarse ensembles C1-C5.

In Fig. 3, we show the impact on X-fits of improving the statistics on the S1 ensemble. We compare 4X3Y-NNLO fits between last year’s statistics and our new results. The corresponding fit parameters are given in Table 2.

Increasing the statistics makes the visual evidence of curvature more convincing and improves the determinations of the LECs. Comparing the S1 results from NLO fits and NNLO fits we see from Table 2) that d_0 and d_1 are consistent, although the latter is poorly determined in both fits.

Fortunately, it is d_0 which gives the dominant contribution to the physical B_K , and this is well determined by both fits.

4. Continuum Extrapolation

Repeating the above procedure on all ensembles yields the results for B_K quoted in Table 1. Here we have run these results to a common renormalization scale, $\mu = 2$ GeV. The next steps are to extrapolate to the continuum limit, and to estimate all sources of error.

We do the continuum extrapolation using the results from the C3, F1, S1 and U1 lattices. These lattices all have the same ratio of sea quark masses, $m_l/m_s = 1/5$ and all have $m_s \approx m_s^{\text{phys}}$. We have seen above that B_K is almost independent of the sea-quark mass, so the lack of exact matching of the sea-quark masses between these ensembles has a very small effect (and can be corrected for).

The expected approach to the continuum limit is somewhat complicated. The dominant errors remaining in B_K are due to taste-conserving discretization errors and errors from the truncation of matching factors. The discretization errors have the form $a^2\alpha_s(1/a)^n$, with $n = 0, 1, 2, \dots$. Note that $n = 0$ is allowed because we do not Symanzik-improve our operators. The truncation errors, by contrast, are proportional to $\alpha_s(1/a)^m$ with $m = 2, 3, \dots$.

Since we cannot hope to disentangle these various dependencies, we adopt a pragmatic approach. We fit to the form

$$B_K(a) = B_K(a=0) + b_1 a^2 + b_2 a^4, \quad (4.1)$$

with or without the quadratic term. This takes care of the dominant a^2 term, and the inclusion of the b_2 is an approximate way of allowing for dependence such as $a^2\alpha_s$. Clearly this fit does not treat the truncation error correctly. Instead, we treat this as a systematic error, as discussed below.

In Fig. 4, we show linear and quadratic fits to the a^2 dependence of B_K . The fits agree well, and we choose the linear fit for our central value and statistical error. We quote the difference between the result on the U1 lattice and the continuum extrapolated value as an estimate of systematic error in the continuum extrapolation (due to our not accounting for $a^2\alpha_s$ terms).

5. Error Budget and Conclusion

cause	error (%)	memo	status
statistics	1.4	4X3Y-NNLO fit	update
matching factor	4.4	$\Delta B_K^{(2)}$ (U1)	update
discretization	0.10	diff. of (U1) and $a = 0$	update
fitting (1)	0.92	X-fit (C3)	[5]
fitting (2)	0.08	Y-fit (C3)	[5]
am_l extrap	0.48	diff. of (C3) and linear extrap	[5]
am_s extrap	0.5	constant vs linear extrap	[5]
finite volume	0.85	diff. of 20^3 (C3) and 28^3 (C3-2)	[5]
r_1	0.14	r_1 error propagation	[5]

Table 3: Error budget for B_K obtained using SU(2) SChPT fitting.

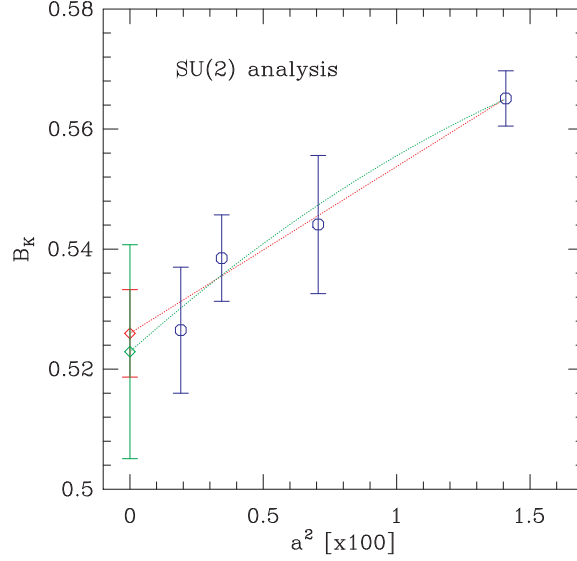


Figure 4: Continuum extrapolation of $B_K(\text{NDR}, \mu = 2 \text{ GeV})$. Linear and quadratic fits to a^2 (in $\text{fm}^2 \times 100$) are shown. The results are from 4X3Y-NNLO SU(2) SchPT fits.

The error budget for the SU(2) analysis is presented in Table 3. Several of the errors are as in Ref. [5], and we refer to that work for explanations and discussion of these errors.³ The errors which have changed since Ref. [5] are those due to statistics (reduced from 1.7%), matching (reduced from 5.5%) and discretization (reduced from 1.8%). Our estimate of the latter error, explained in the previous section, may be an underestimate, but in any case is dominated by the matching error.

The matching error is estimated as follows. We assume that the dominant missing term in the perturbative matching factors is of size $1 \times \alpha_s^2(\mu = 1/a)$, so that the error in B_K is

$$\Delta B_K^{(2)} \approx B_K^{(1)} \times \left[\alpha_s(1/a) \right]^2, \quad (5.1)$$

where $B_K^{(1)}$ is the result using one-loop matching. This error will be reduced, but not eliminated, by the continuum extrapolation. To be conservative, we take as the error the size of $\Delta B_K^{(2)}$ on our smallest lattice spacing. The reduction in this error compared to Ref. [5] is simply due to our having another, smaller, lattice spacing.

Combining the errors in the error budget, we find

$$\begin{aligned} B_K(\text{NDR}, \mu = 2 \text{ GeV}) &= 0.5260 \pm 0.0073 \pm 0.0244 \\ \hat{B}_K = B_K(\text{RGI}) &= 0.720 \pm 0.010 \pm 0.033. \end{aligned} \quad (5.2)$$

Our result is in agreement with those obtained using valence DWF on either MILC [11] or DWF lattices [10, 12]. Our total error of 5% is somewhat larger than the 4.1% and 3.3% attained in the other calculations, the difference being mainly due to our use of one-loop, rather than non-perturbative, matching.

³See also the companion proceedings [3] for additional discussion of errors due to finite-volume effects and the dependence on sea-quark masses.

6. Acknowledgments

C. Jung is supported by the US DOE under contract DE-AC02-98CH10886. The research of W. Lee is supported by the Creative Research Initiatives Program (3348-20090015) of the NRF grant funded by the Korean government (MEST). The work of S. Sharpe is supported in part by the US DOE grant no. DE-FG02-96ER40956. Computations were carried out in part on QCDOC computing facilities of the USQCD Collaboration at Brookhaven National Lab. The USQCD Collaboration are funded by the Office of Science of the U.S. Department of Energy.

References

- [1] Hyung-Jin Kim, *et al.* PoS (LATTICE 2009) 262; [arXiv:0910.5573].
- [2] Jangho Kim, *et al.* PoS (LATTICE 2010) 310; [arXiv:1010.4779].
- [3] Yong-Chull Jang, *et al.* PoS (LATTICE 2010) 229; [arXiv:1010.4780].
- [4] Taegil Bae, *et al.*, PoS (Lattice 2010) 296; [arXiv:1010.4781].
- [5] Taegil Bae, *et al.*, [arXiv:1008.5179].
- [6] Weonjong Lee and Stephen Sharpe, Phys. Rev. D **60** (1999) 094503, [hep-lat/9905023].
- [7] C. Aubin and C. Bernard, Phys. Rev. D **68** (2003) 034014, [hep-lat/0304014].
- [8] R.S. Van de Water and S.R. Sharpe, Phys. Rev. D **73** (2006) 014003, [hep-lat/0507012].
- [9] A. Roessl, Nucl. Phys. B **555**, 507 (1999) [hep-ph/9904230].
- [10] C. Allton *et al.* [RBC-UKQCD Collaboration], Phys. Rev. D **78**, 114509 (2008) [arXiv:0804.0473 [hep-lat]].
- [11] C. Aubin, J. Laiho and R. S. Van de Water, Phys. Rev. D **81**, 014507 (2010) [arXiv:0905.3947 [hep-lat]].
- [12] C. Kelly, P. A. Boyle and C. T. Sachrajda [RBC Collaboration and UKQCD Collaboration], PoS **LAT2009**, 087 (2009) [arXiv:0911.1309 [hep-lat]].